Failure detection and control for wire EDM process using multiple sensors

Abhilash P. M.*, D. Chakradhar

Department of Mechanical Engineering, Indian Institute of Technology Palakkad, Kerala, India, 678557

*Corresponding author: abhilashpm184@gmail.com, ORCID ID: 0000-0001-5655-6196

Abstract: Unstable machining conditions during wire EDM process would lead to process failures, affecting the efficiency and sustainability of process. The study aims to develop a sensor-based failure prediction and process control system. The monitoring system consisting of high sampling rate differential and current probes extracts voltage and current signals during spark machining. Relevant discharge characteristics like pulse proportions, pulse frequency, and discharge energy are extracted from the pulse train data. The proposed process control algorithm works in three stages: failure prediction, failure severity assessment, and process control. Failure conditions considered are wire breakage and spark absence, which are predicted based on the extracted discharge characteristics. Severity of failure is judged based on the spark discharge energy. The proposed process control algorithm retunes the process parameters by adjusting pulse on time, pulse off time, and servo voltage, based on the type of failure and its severity. The methodology was successful in preventing the potential failure situation by restoring the machining stability. This was demonstrated by conducting confirmation experiments. Microstructural comparison of machined surfaces and worn wire surfaces also confirms the effectiveness of the proposed strategy to ensure failure free machining with better surface integrity.

Keywords *Wire-EDM; process failure; wire breakage; condition monitoring; process control; adaptive control*

1. Introduction

Wire electric discharge machining (wire EDM) is a non-conventional machining process which possesses several advantages over conventional machining due to the non-contact nature of material removal. Here, the mechanism of material removal involves melting and vaporisation by controlled electric sparks (Ho et al., 2004). Sparks happens between a conductive wire electrode and workpiece separated by a dielectric medium. On application of a voltage across the electrodes, the dielectric ionises and a discharge spark is produced between the electrodes. The temperature in the machining zone will be high enough to melt any material, thus making it possible to machine any conductive materials irrespective of their hardness (Mandal and Dixit, 2014). Even though the process exhibits such immense potential, controlling the process stability has always been challenging. Unstable machining conditions has resulted in process failures like wire breakages leading to material and energy wastage (Gamage and Desilva, 2016). To improve the process sustainability and efficiency, process

This is a peer-reviewed, accepted author manuscript of the following article: P. M., A., & Chakradhar, D. (2021). Failure detection and control for wire EDM process using multiple sensors. CIRP Journal of Manufacturing Science and Technology, 33, 315-326. https://doi.org/10.1016/j.cirpj.2021.04.009

failures have to be predicted and controlled. Also, to improve the productivity and surface integrity of machined parts, process interruptions by wire breakages have to be eliminated.

Many researchers have observed that the selection of non-ideal parameter combinations is a prominent reason for process failures. Many works on process optimization of superalloys and Ti alloys were attempted in this regard (Hewidy et al., 2005; Gautier et al., 2015; Aggarwal et al., 2015; Senkathir et al., 2019). However, process optimization alone is not sufficient to completely eliminate the process interruptions by wire breakages. This is because of the stochastic nature of the process, complex interaction effects, and interference of uncontrollable factors (Abhilash and Chakradhar, 2020). In order to eliminate wire breakages, it is important to understand the wire wear mechanism leading to rupture. Cabanes et al. (2008) observed that the wire breakages are associated with poor flushing, coupled with varying discharge frequency. Fedorov et al. (2008) categorised the wire breakage mechanism into implicit and explicit. Unideal short circuit sparks and debris accumulation by ineffective spark gap control were recognised as the chief causes of wire breakages. Through CFD simulations, Okada et al. (2015) found that the stagnation of debris in the inter electrode gap leading to wire vibrations is the main cause of wire breakage. Shorter than ideal spark gap increases the tendency of spark gap bridging, which leads to higher wire breakage frequency.

Earlier attempts on condition monitoring were based on spark frequency (Rajurkar and wang, 1991), discharge energy of sparks (Kwon and Yang, 2006), and wire strength (Luo, 1999). A few fuzzy logic-based control strategies were also developed. Yan and Liao (1996) developed a fuzzy logic system to predict wire breakages by tracking the sparking frequency. Two types of wire break phenomena were reported based on sudden spark frequency rise and gradual spark frequency rise. Liao and Woo (2000) designed a control system based on short circuit spark proportion and power level. Pulse off time was tuned by the controller to regulate short circuit sparks. Fuzzy logic-based accuracy control was attempted by Li et al. (2001). Bufardi et al. (2015) attempted a fuzzy control system in which an offline model sets the initial parameters and an online model performs real time process control. Offline models to predict process failures during wire EDM of Inconel 718 was developed using ANN classification (Abhilash and Chakradhar, 2020), ANFIS (Abhilash and Chakradhar, 2020) and Naïve bayes classifier (Abhilash and Chakradhar, 2021).

Modern condition monitoring systems are pulse classification-based systems. Different pulse classification algorithms are developed by Janardhan and Samuel (2010), Obwald et al. (2018) and Conde et al. (2018). Kwon and Yang (2006) developed a model to predict process stability based on instantaneous energy. The developed system alerts the user during unstable

conditions, but a control strategy was not proposed. Newton et al. (2009) developed a regression model to predict the recast layer thickness using the extracted pulse parameters. A regression model, however, requires prior knowledge of the type of input output relationship function and thus can be inaccurate. Through regression, it is difficult to model non linearities in higher dimensions. Klocke et al. (2014) developed a monitoring model to track the surface roughness during the fir tree slot machining of Inconel 718. The proposed model extracts mean voltage difference between the electrodes, and this parameter was considered as an indicator of the surface quality. The work, however, have not considered the effect of the current signals in the analysis. Caggiano (2015) proposed extraction methodology for multiple discharge characteristics to identify and predict machined part quality. Mwangi (2020) studied the effect of arching on process failure and part quality during micro EDM of Nitinol.

It was evident from the literature survey that the existing models for wire EDM failure prediction and process control leaves a few key areas unaddressed. The existing statistical models to predict wire breakages (Kumar and Choudhury, 2011; Kumar et al., 2013) can be inaccurate and unreliable since they just map inputs and responses and does not consider the process data. This is very critical for a stochastic process like wire EDM, where several external uncontrollable factors can affect the failure mechanism. The fuzzy logic methods (Yan and Liao, 1996; Bufardi et al., 2015; Liao and Woo, 2000) are expert knowledge dependent and not trainable. Also, most of the developed monitoring systems can only alert the users regarding failures, but cannot perform process control to restore machining stability (Kwon and Yang, 2006; Cabanes et al., 2008). Also, while most of the previous process control models (Liao and Woo, 2000; Cabanes et al., 2008; Bufardi et al., 2015) focuses only on the wire breakage prevention, the current study is aimed at preventing multiple process failures.

The proposed failure prediction and process control system is a systematic, data driven approach which does not requires empirical modeling. Such a model does not require prior knowledge of the process mechanisms or the effect of process parameters on the responses. The study introduces a novel three step procedure for wire EDM process control which involves - failure prediction, severity assessment and optimal parameter regulation. A data driven model which minimizes the shortcomings of the existing models discussed thus far is being proposed. The objective of the current study are as follows:

- To develop a failure prediction algorithm based on the extracted discharge characteristics
- To propose a systematic control strategy to regulate the process parameters to prevent machining failures based on the type and severity of the predicted failure

2 Materials and Methods

2.1 Materials

Inconel 718 is a nickel-based superalloy known for its high performance at elevated temperatures. The excellent mechanical strength, fatigue and creep resistance of the alloy is utilized in aerospace applications. The alloy is considered difficult to cut using conventional processes and thus wire EDM is considered as a suitable alternative due to its non-contact material removal mechanism. The mechanical properties and chemical composition of Inconel 718 is given in Table 1 and Table 2 respectively.

Table 1 Properties of Inconel 718 (Thakur, 2009)

Property	Value
Density	8.19 g/cm^3
Melting Point	1260 – 1336 ^{o}C
Specific Heat	435 J/kg K
Average Coefficient of thermal expansion	13 μm/m K
Thermal Conductivity	11.4 W/m K
Ultimate Tensile strength	1240 MPa

Table 2 Chemical composition of Inconel 718 (Reed, 2006)

Element	Ni	Fe	Cr	Nb	Mn	C	Co	Al	Si	Ti	Mo	Others
Weight (%)	51.05	19.43	18.70	5.7	0.07	0.04	0.2	0.56	0.08	1.01	3.1	0.06

2.2 Experimental plan

Electronica Ecocut wire ED machine is used to perform the experiments. The machine is having a resolution of 1 μm in every axis. Dielectric fluid considered for the study is deionised water. Since zinc coated electrodes are reported to have better overall performance than uncoated electrodes (Maher et al, 2014; Ramamurthy et al., 2015), hard zinc coated brass wires of diameter 0.25 mm and tensile strength 900 N/mm 2 is chosen as the wire electrode. The profile machined for this experimental study is straight cut of length 50 mm. The profile is made on an Inconel plate of thickness 10 mm. Experiments are repeated thrice to rule out experimental errors.

A current sensor (Make: Tektronix, Model: TCP 303, country: US) and current probe amplifier (Make: Tektronix, Model: TCP 300, Country: US) constitute the AC/DC current

measuring system used in this study. The sensor is having a bandwidth of 15 MHz and the measuring range is from 5mA to 150A RMS at high current range. A voltage sensor (Make: Tektronix, Model: P 5200A, Country: US) having variable bandwidth and attenuation is equipped to the wire EDM for real time voltage measurement. The sensor has a measuring range of ± 1300 V and a 50 MHz bandwidth. An oscilloscope (Make: Tektronix, Model: MDO 34-200, Country: US), having maximum sampling rate of 2.5 G sa/s on all channels is used to record the measured waveforms. The signals were recorded for 20 ms with 250 million samples/second sampling rate.

The parameters and ranges are selected based on pilot experiments, literature review, and operator's manual, and authors' previous experimental studies to develop offline models (Abhilash and Chakradhar, 2020; Abhilash and Chakradhar, 2021). The pilot experiments were one factor at a time experiments, where the failure condition is observed with respect to an input parameter keeping every other parameter constant. The parameters which were found to have higher influence on machining failures are considered for this study. The safe limits and failure conditions were realized for each input parameter through such experiments. The parameter combinations given in Table 3, are deliberately selected to cause machining failures like wire breakages, since the study aims to study failure occurrence. Signal processing and analysis are performed in Matlab 2019 software. Zeiss scanning electron microscope (Model: GeminiSEM, Country: Germany) is used for microstructural study. AEP non-contact surface profilometer (Model: Nanomap, Country: US) is used to capture surface morphological images.

Table 3. Process parameters and levels

Parameters	**Pulse on time** T_{on} (μs)	**Pulse off time** T_{off} (μs)	**Servo voltage** SV (V)	**Input current** I_p (A)
Level 1	105	30	30	40
Level 2	110	40	50	10
Level 3	115	50		

2.3 Measurement setup and signal processing

The configuration of the monitoring setup is shown in Fig. 1. Fig. 2 shows the multi sensor setup for the conduction of the experiments. The raw signals captured by the differential probe and current probe are filtered by the 'signal analyser' tool in Matlab. Then the required features like discharge energy, ignition delay time, sparking frequency are extracted. Furthermore, using the proposed algorithm, the proportion of different pulses are extracted from the filtered waveform. Pulse ratios like arc spark ratio, short circuit spark ratio, open spark ratio, and normal spark ratio are found. Useful conclusions regarding the process stability and performance can be drawn from these extracted features. This methodology of pulse train analysis for wire EDM process control is shown in Fig. 3.

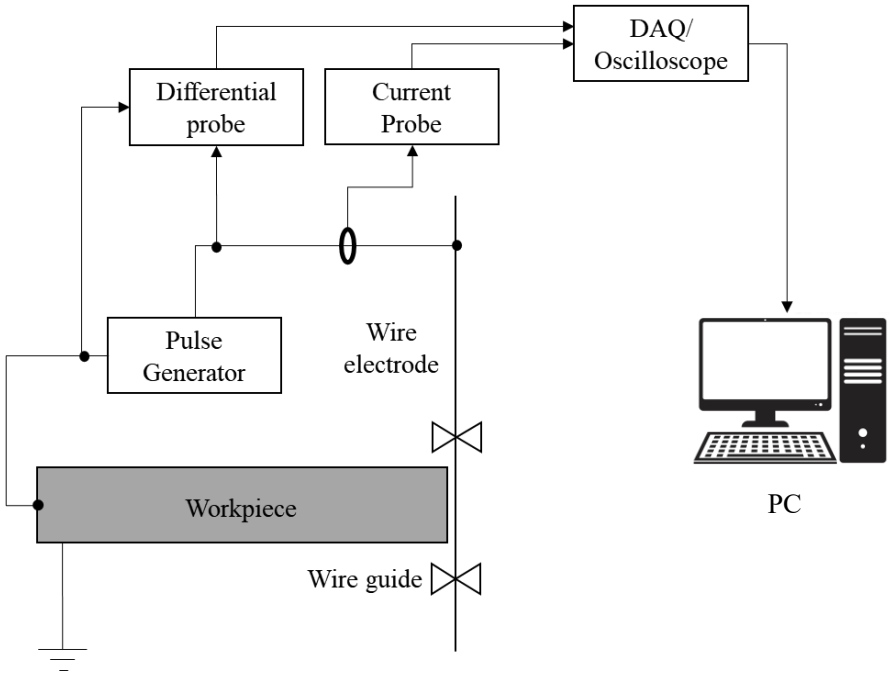

Fig. 1. Schematic arrangement of the pulse measurement setup

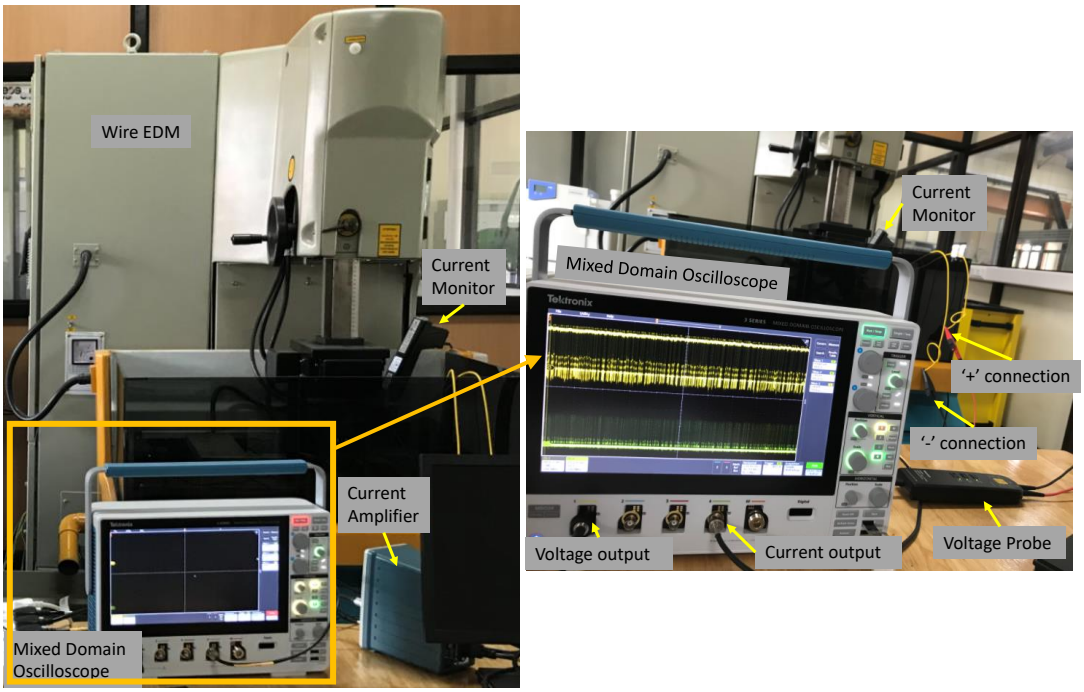

Fig. 2. Experimental setup for the pulse-train acquisition system

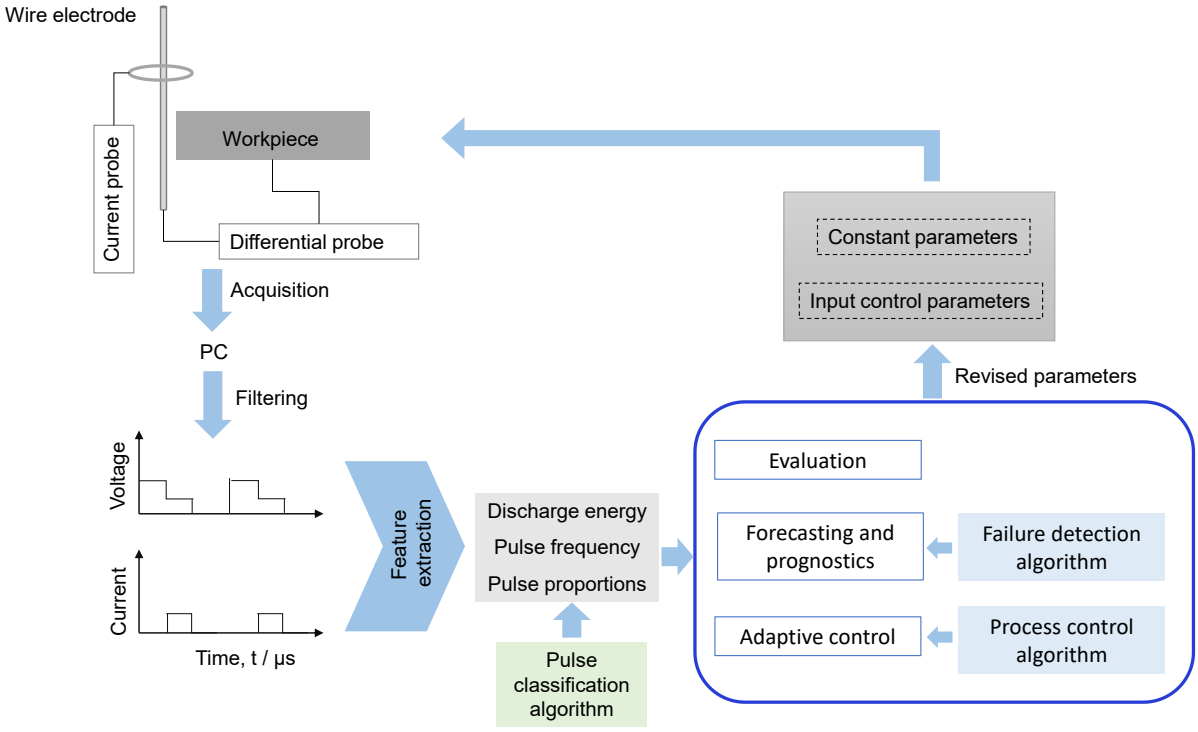

Fig. 3. Process control strategy

2.4 Pulse classification

Wire EDM pulses are classified into normal, open, arc, and short circuit discharges (Caggiano, 2015). The shapes of various discharge pulses are shown in Fig. 4. A pulse classifier

and counter are used to calculate the proportion of each pulse types in the recorded time period. Pulse proportions are useful indicators of the process stability (Conde et al., 2018). Arc discharges are the ones with negligible ignition delay time. Higher proportion of arc discharges indicates increased conductivity of spark gap dielectric due to suspended debris. Short circuit discharges are an extreme condition of arc discharge in which the discharge happens without a voltage pulse peak. Short sparks happen when the gap is bridged with accumulated debris (Caggiano et al., 2015). Higher proportion of open circuit pulses indicates a larger spark gap. Increased percentage of arc or short sparks results in poor part quality and wire break failure (Cabanes et al, 2008).

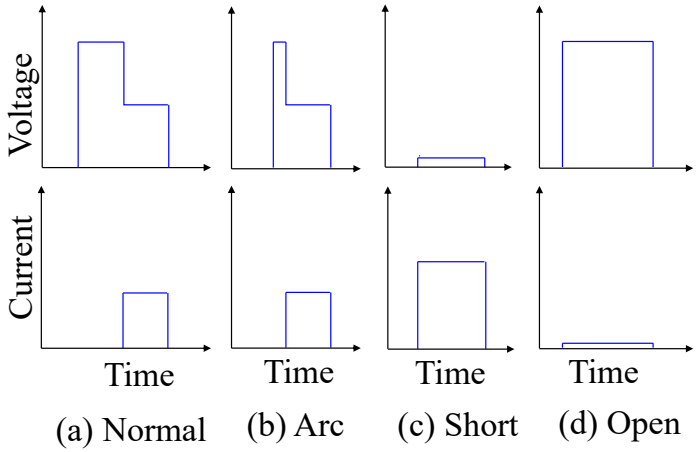

Fig. 4. Classification of discharge pulses

The proposed process control system accesses the process health by monitoring the behaviour of health indicators. The health indicators of the wire EDM process are the discharge characteristics like abnormal spark ratio, discharge energy, and sparking frequency. The system monitors the process health based on these extracted features to predict risks of process failures. Also, the system detects the severity of process instability and re-tune the process parameters to ensure failure free machining using a process control algorithm. The data flow in the proposed system is shown in Fig. 3.

3. Results and Discussion

Different cases of machining outcomes are considered for assessing the performance of the proposed intelligent process control system. Machining failure is defined when any of the following cases occurs (a) when the process fails to perform the required function, or (b) when a breakdown event causes an interruption (Tung et al., 2009). In the case of wire EDM process, former case corresponds to spark absence and later case is when the wire breaks. Spark absence

is an inefficient machining situation where the discharge energy is too less to break the dielectric barrier to produce sustained repetitive sparks (Abhilash and Chakradhar, 2020). This can also happen when the spark gap is too high. However, wire breakage failure, caused by the accumulation of machining instabilities, is regarded as more critical due to its higher impact on productivity, and its detrimental effects on machined profile (Gamage and Desilva, 2016). Such failures can be detected well in advance from the pulse characteristic features, which are investigated in this study. The proposed failure detection and process control algorithm is discussed in the subsequent sections.

3.1 Failure detection and control algorithm

During the pulse cycle analysis, the different types of pulses identified are shown in Fig. 5. Fig. 6 and Fig. 7 shows the discharge patterns leading to failure cases. In the case of wire break failures, it can be observed from Fig. 6 that the proportion of arc and short circuit discharges are significantly higher than the normal discharges. Also, since short sparks happens without an ignition delay period, the sparking frequency was observed to be extremely high. Similar observation was reported by Cabanes et al. (2018), Kwon et al. (2015) and Bergs et al. (2018). Again, since higher energy discharges are the root cause of excess debris, gap bridging and short sparks, the discharge energy of sparks are found to be significantly higher than the normal case. It was observed that occurrence of just one of the above situations need not cause wire breakage.

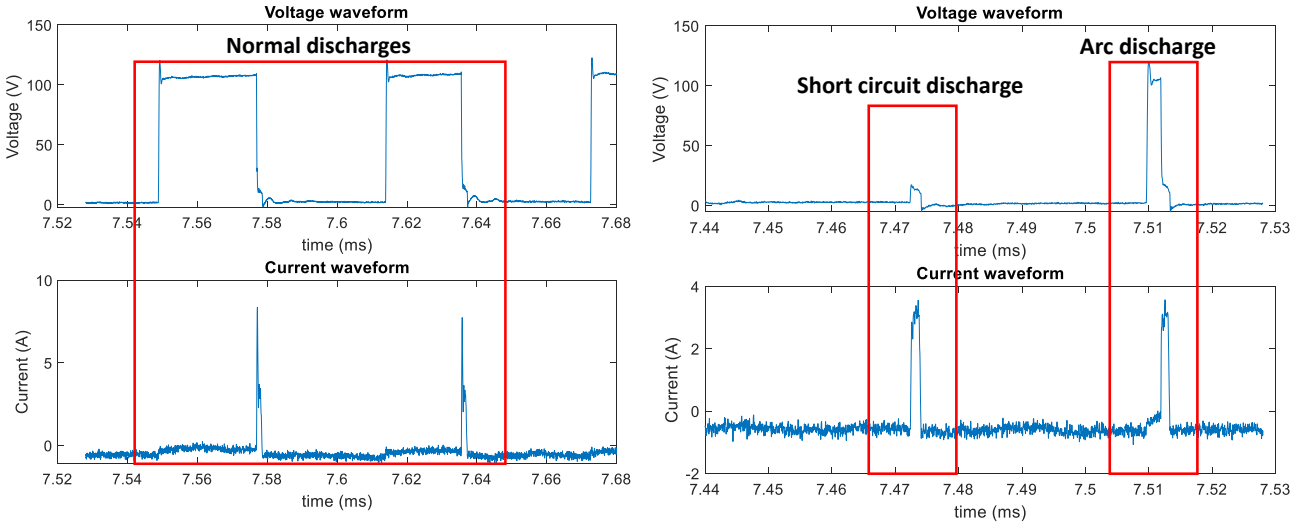

Fig. 5. Different types of discharge pulses

Fig. 7 shows the other extreme when the sparks die out when the dielectric properties in the inter electrode gap is not suitable to sustain repeated sparks. The situation arises when the open circuit voltage is not high enough to ionise the dielectric to form an electric arc across

electrodes, as reported previously by Abhilash and Chakradhar (2020). Here most of the sparks are open circuit sparks, where discharge current is absent. Due to this, the spark frequency is extremely low, even less than 1000 Hz in most cases. Also, the discharge energy of individual sparks is extremely less.

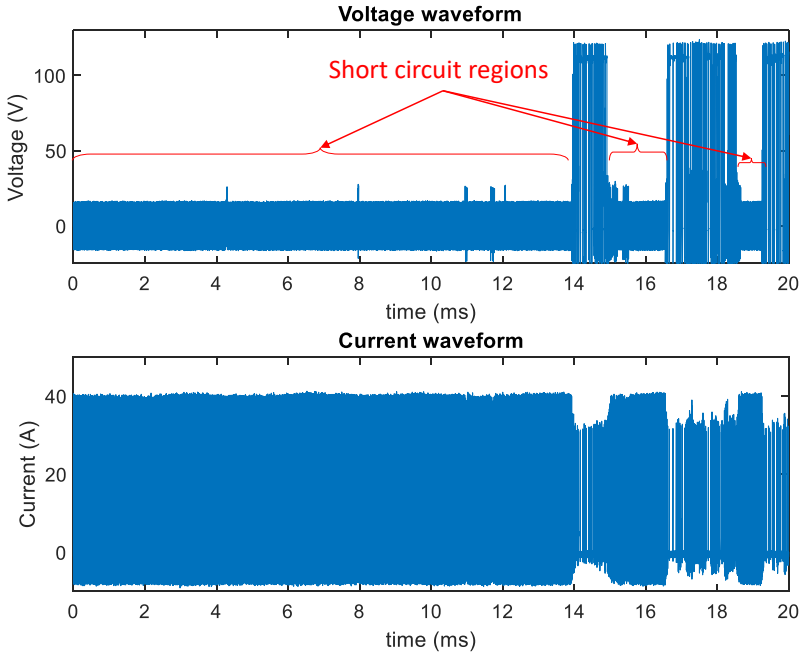

Fig. 6. The pulse cycle behaviour leading to wire breakage failure

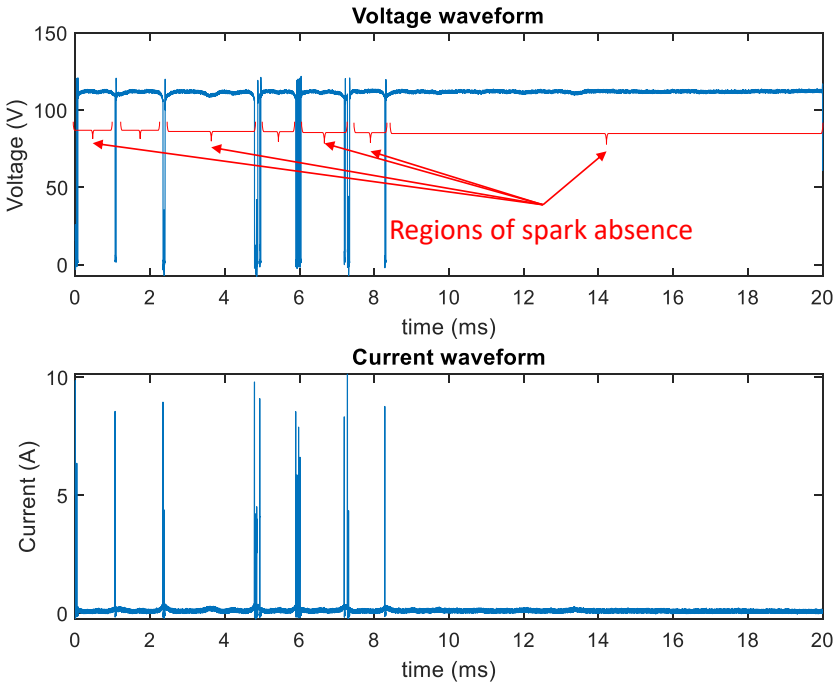

Fig. 7. The pulse cycle behaviour leading to spark absence case

The proposed failure prediction and control algorithm works in three steps.

Step 1 – Failure prediction: Based on the pulse cycle behaviour and the values of discharge characteristics leading to process failures, a logic for failure prediction was formulated. The discharge characteristics considered are various pulse proportions, discharge energy and spark frequency. The threshold values of discharge characteristics are formulated heuristically by conducting 36 experiments, each of which are replicated thrice. Here, unideal input parameter combinations are consciously selected to result in machining failures. Table 4 and Table 5 shows the cases of wire breakage and spark absence with corresponding extracted features.

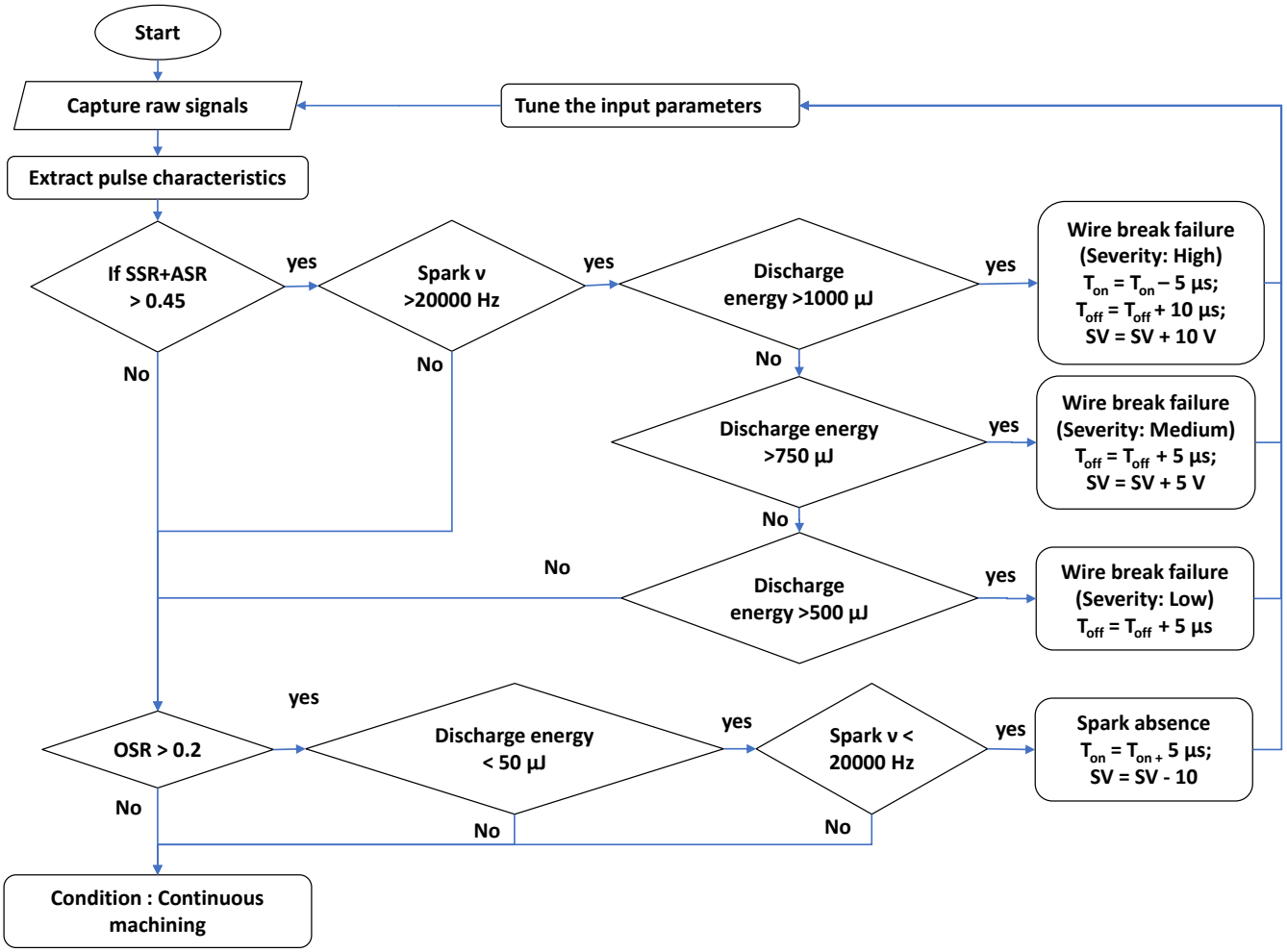

Fig. 8. Flowchart of failure detection and control method

Step 2 – Assessment of failure severity: The control algorithm is coded based on the failure detection rules. Once wire breakage is forecasted, its severity is identified based on the average discharge energy of sparks. Discharge energy is chosen as an indicator of the severity of spark gap instability based on a wire wear study conducted by Abhilash and Chakradhar (2020). It was revealed that higher discharge energy sparks resulted in accelerated wire wear and can lead to faster wire rupture. The most severe case is when the wire electrode ruptures very soon after the commencement of the machining. This case is identified by an extreme high discharge

energy. Machining instability was classified into three categories, based on the discharge energy values.

Step 3 – Process control: Once the failure condition and severity are predicted, next step is to suggest alternate input parameter settings to restore the machining stability. For this purpose, pulse on time, pulse off time and servo voltages are adjusted based on the detected condition. The overall detection and control algorithm are given in Fig. 8.

Table 4. Extracted discharge characteristics leading to wire break failure

S. No	Input parameters				Extracted signal features			Observed failure
	Pulse on time (μs)	Pulse off time (μs)	Servo voltage (V)	Input current (A)	SSR + ASR	Spark ν (Hz)	Discharge energy (μJ)	
1	105	30	30	40	0.84	75000	613.68	Wire breakage
2	110	30	30	40	0.43	26500	1044.30	
3	110	30	50	40	0.44	45000	1066.32	
4	110	40	50	40	0.53	29000	986.55	
5	110	50	50	40	0.54	20500	1002.03	
6	115	30	30	40	0.59	22500	1476.84	
7	115	40	30	40	0.75	25500	1484.71	

ASR- Arc spark ratio, SSR- Short spark ratio

Table 5. Extracted discharge characteristics leading to spark absence failure

S. No	Input parameters				Extracted signal features			Observed failure
	Pulse on time (μs)	Pulse off time (μs)	Servo voltage (V)	Input current (A)	Open spark ratio	Spark ν (Hz)	Discharge energy (μJ)	
1	105	40	50	10	0.58	12000	47.62	Spark absence
2	105	50	30	10	0.31	13500	32.06	
3	105	50	50	10	0.44	19500	42.60	
4	110	50	50	10	0.45	14500	42.55	
5	115	50	50	10	0.48	15500	65.58	

A comparison of discharge characteristics at different machining conditions are shown in Fig. 9. The ideal stable spark gap conditions will lead to uninterrupted and continuous machining, whereas the unstable conditions are identified by its deviations from the expected discharge characteristics. Machining instability causes process failures or interruptions through wire breakage and spark absence (Kwon and Yan 2006). One indication of an approaching wire breakage is increased spark frequency. Wire breakage is mainly caused by debris stagnation in

the inter electrode volume which results in ignition delay free sparks (Cabanes et al., 2008; Okada et al, 2015). Frequency of such sparks are higher than normal, since the time delay to ionize the dielectric and break the dielectric barrier is negligible in this case. On the contrary, if the conductivity is too less or the spark gap is too high for the applied voltage to ionize and cross the dielectric barrier, spark frequency will be very less. Such situations can lead to process interruptions by spark absence (Abhilash and Chakradhar, 2020). Also, the discharge energy of sparks leading to wire break failure are more than normal. It was also observed that the proportion of short and arc pulses are significantly higher before wire breakage. Similarly, the proportion of open circuit pulses are more before the spark absence situation.

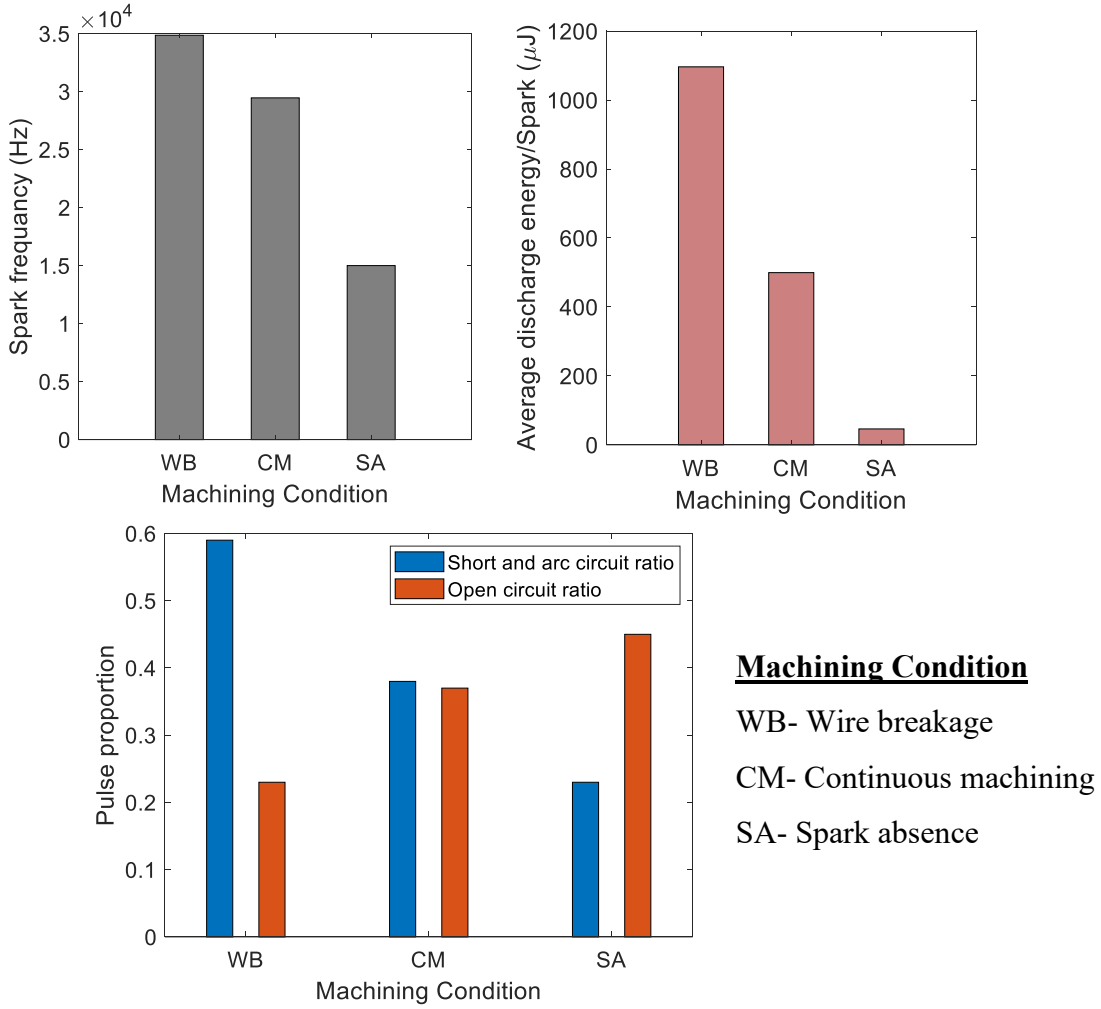

Fig. 9. Average values of pulse characteristics at different machining conditions

3.2 Effects of process control

The effects of revised parameters on the discharge characteristics and machining outcome are shown in Table 6. The process failures are predicted and eliminated by the proposed algorithm. The process control ensured a continuous and stable machining. The discharge

characteristics which were unideal earlier are brought back to the normal levels. A comparison of discharge pulse cycle before and after process control are shown in Fig. 10 and Fig. 11. The waveform data are taken from experiment number 1 and 5 from Table 6. The predominance of short circuit sparks and open circuit sparks in the pulse train are replaced with normal discharge sparks. In case of wire break prediction, depending on the degree of instability, the algorithm lowers pulse on time and increases pulse off time and servo voltage. By doing so, the debris amount is reduced, additionally, time to flush off the debris and the spark gap are increased. The cumulative effect is the avoidance of debris stagnation in the spark gap, which eliminates the wire break failure. Similarly, in case of spark absence prediction, spark gap is narrowed by adjusting the servo voltage. This eases the ionization of dielectric in the spark gap, ensuring sustained repetitive normal discharges. The process control algorithm thus restores the machining stability and ensures failure free continuous operation.

Table 6. Comparison of machining outcomes before and after process control

S. No	Condition	Input parameters				Extracted signal features				Machining outcome	R_a (μm)
		T_{ON} (μs)	T_{OFF} (μs)	Servo voltage (V)	I_P (A)	ASR + SSR	OSR	Spark ν (Hz)	Discharge energy (μJ)		
1	Initial	113	30	35	40	0.97	0	84600	1569	WB	3.47
	Controlled	108	40	55	40	0.08	0.08	9650	433	CM	2.37
2	Initial	115	32	33	40	0.92	0.01	61200	1705	WB	3.31
	Controlled	110	42	43	40	0.10	0.24	7600	503	CM	2.43
3	Initial	110	33	31	40	0.79	0.01	21350	990	WB	3.12
	Controlled	110	38	36	40	0.18	0.18	7700	87	CM	2.29
4	Initial	112	30	30	40	0.83	0	62500	559	WB	3.37
	Controlled	112	35	30	40	0.23	0.21	7450	102	CM	1.96
5	Initial	105	50	48	10	0.17	0.5	300	59	SA	-
	Controlled	110	50	38	10	0.24	0.01	3215	24	CM	0.96
6	Initial	107	45	50	10	0.36	0.64	550	49	SA	-
	Controlled	112	45	40	10	0.26	0	3015	27	CM	0.83

WB – Wire breakage, CM- Continuous machining, ASR- Arc spark ratio, SSR- Short spark ratio, OSR- Open spark ratio

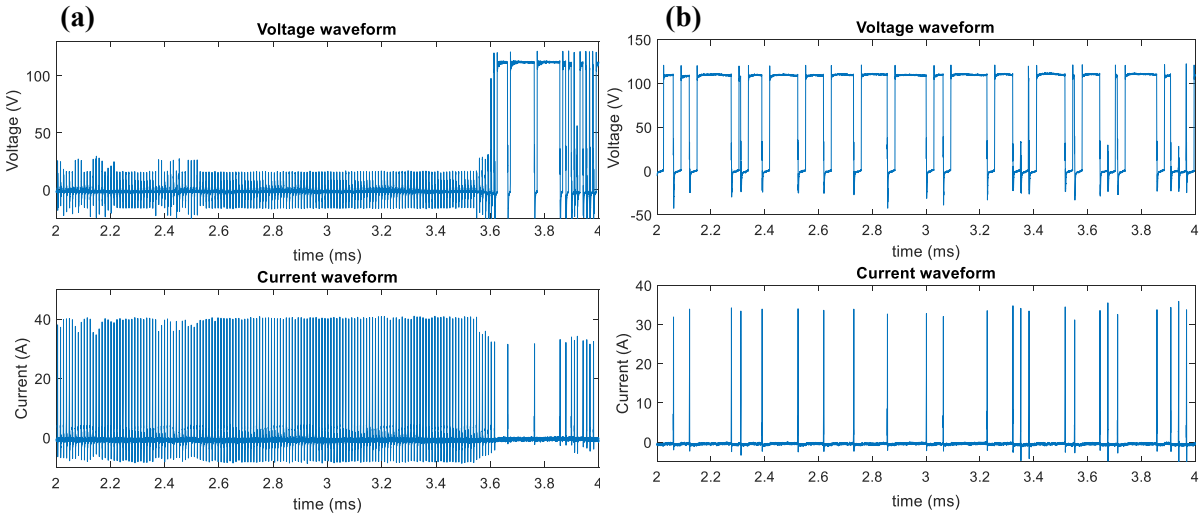

Fig. 10. Discharge pulse waveform (a) leading to wire breakage (b) after parameter tuning based on the control algorithm

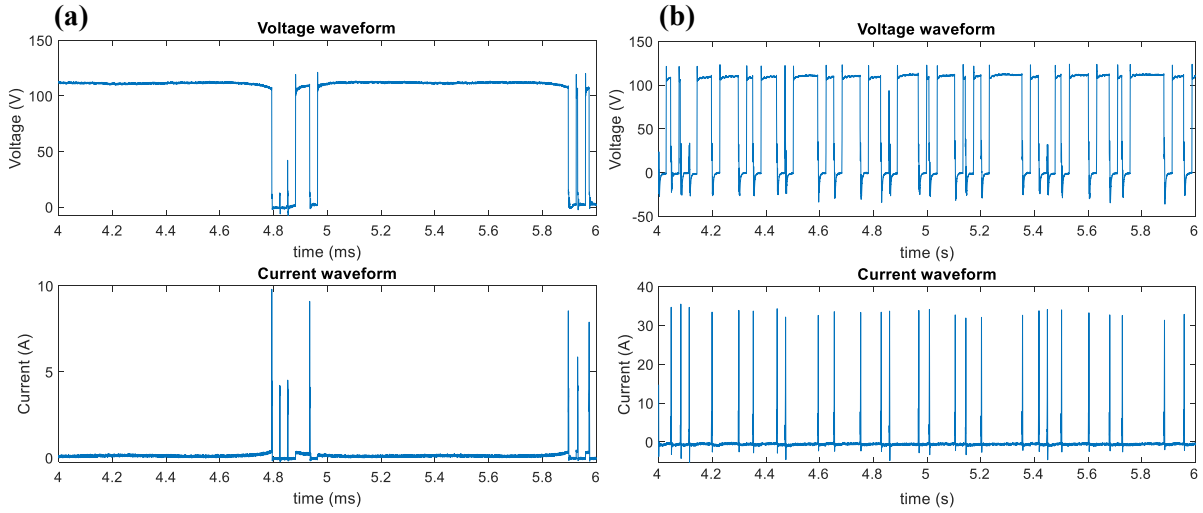

Fig. 11. Discharge pulse waveform (a) leading to spark absence (b) after parameter tuning based on the control algorithm

In order to compare the extend of wire wear phenomena before and after process control, SEM images of worn wire samples are compared. Severe wire surface degradation is observed due to undesirable sparks leading to wire breakage (Fig. 12 (a)). Once the wire degradation crosses a limit, the wire will no longer be able to bear the axial wire tension. At this point, the wire will start to elongate at the point of maximum wear by reducing the wire cross section (Pramanik and Basak, 2017). The ruptured wire is thus found with a conical tip, having debris impinged to the surface, and a visible melt pool (Fig. 12 (b)). After process control, the wire wear has substantially reduced, with only minimal visible degradation to the wire surface (Fig.

12 (c)). Exp. No.1 of confirmation test is considered to demonstrate the effect of process control on wire wear.

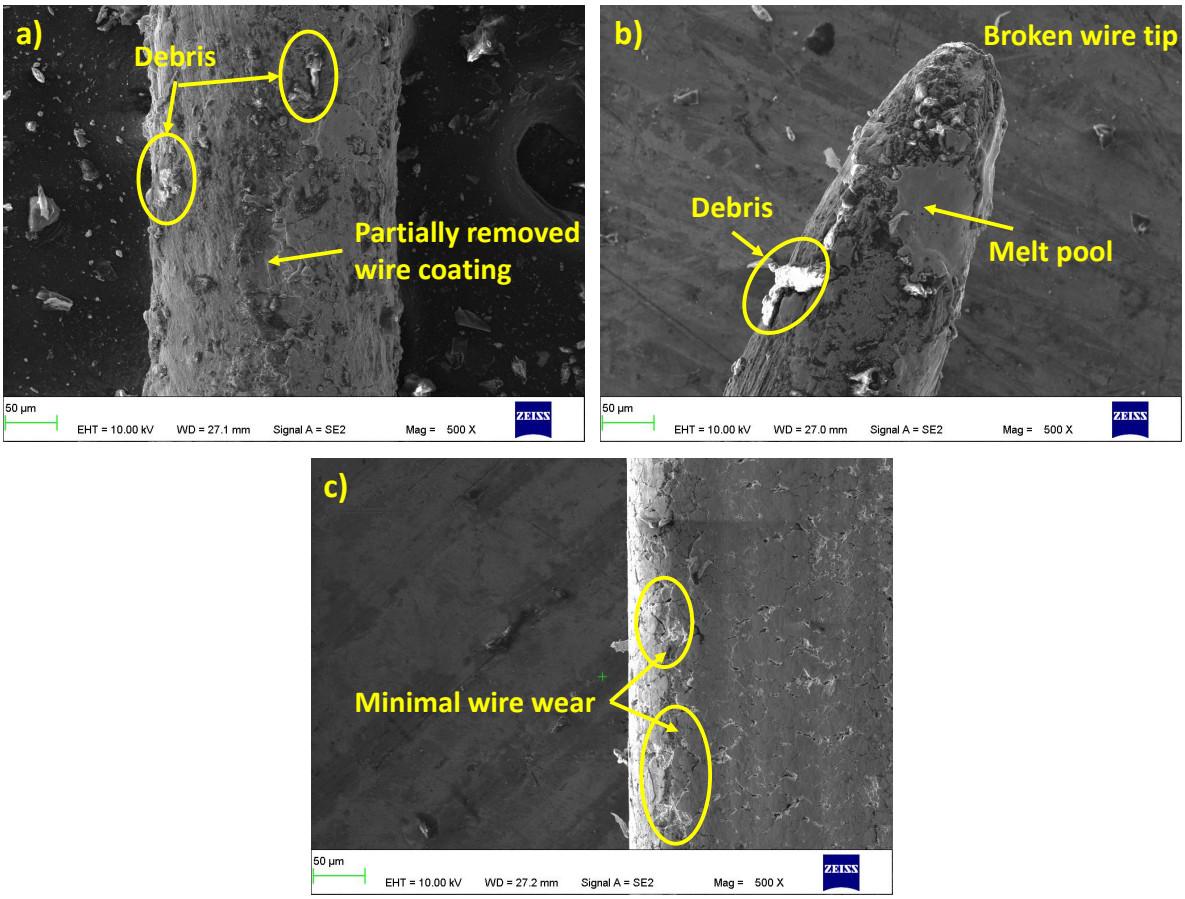

Fig. 12. (a) Worn wire surface leading to wire breakage (b) broken wire tip (c) worn wire after process control

The proposed process control algorithm, not only ensures a failure free operation by adjusting the parameters, but is observed to enhance the surface integrity of the machined components. The average surface roughness, R_a was observed to improve under controlled process condition. Process conditions leading to wire breakage can cause surface defects and coarser surface due to higher intensity short circuit sparks. This is shown in Fig. 13. Here, the SEM image of machined surfaces before and after process control are compared for the case of Exp. No. 1 in confirmation tests. The original settings had led to numerous undesirable surface features like micro pits, voids, globules and pores. In comparison, process control has led to a smoother surface with no visible micro defects. The surface morphological changes are also compared using non-contact 3D surface profilometer images as shown in Fig. 14. The original parameter settings leading to wire breakage can be viewed with high peaks and deep valleys, whereas after process control, the surface is more even and smooth.

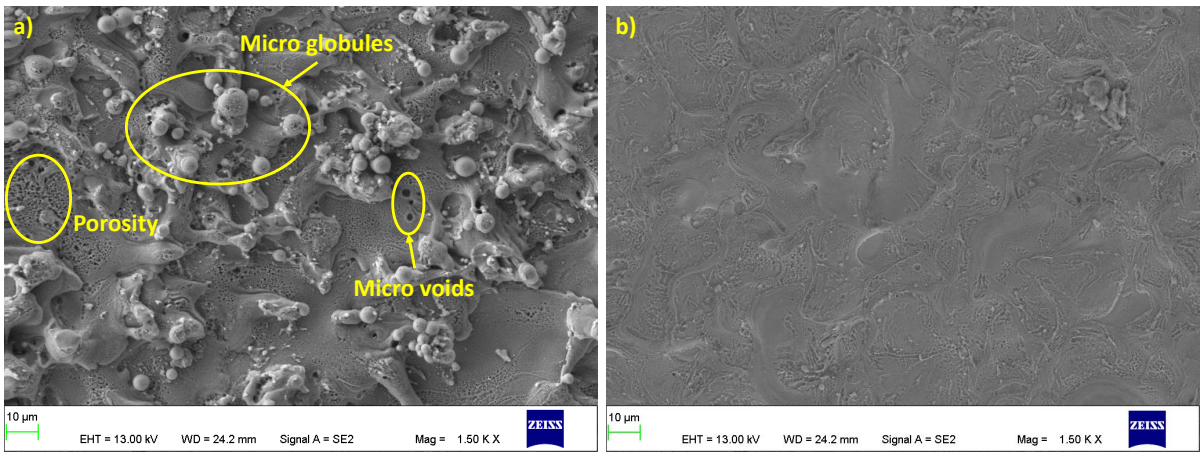

Fig. 13. SEM image of machined surface (a) under original settings (b) after process control

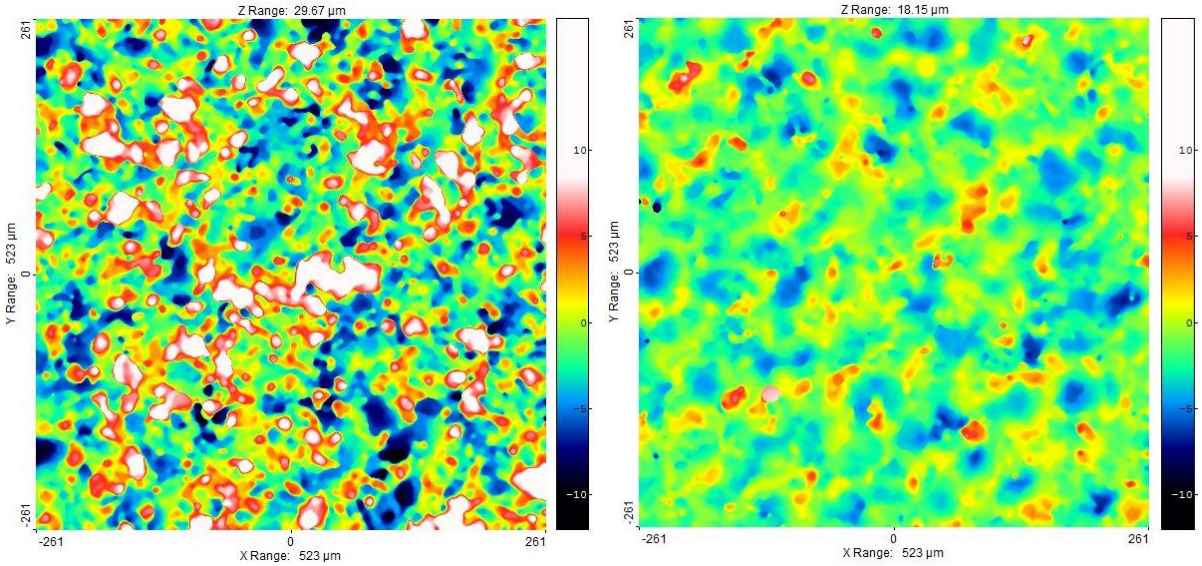

Fig. 14. Non-contact 3D profilometer image of machined surface (a) under original settings (b) after process control

The surface roughness of the machined surface is mostly dependent on the discharge energy of the individual sparks. Each spark is responsible for removing a small portion of workpiece material through melting and vaporisation in the form of micro craters (Sharma et al., 2015). The machining happens by the overall effect of such individual sparks which happens at over 1000 Hz frequency. Higher discharge energy sparks are capable of removing more material from the work surface by forming deeper craters. The deeper the individual craters are, coarser will be the surface morphology (Sharma et al., 2015). A graph showing the effect of discharge energy on surface roughness given in Fig. 15 supports this claim. Also, since it is observed that the short circuit and arc sparks have higher discharge energy, the surface machined by short/arc dominant pulse cycle is also of inferior part quality.

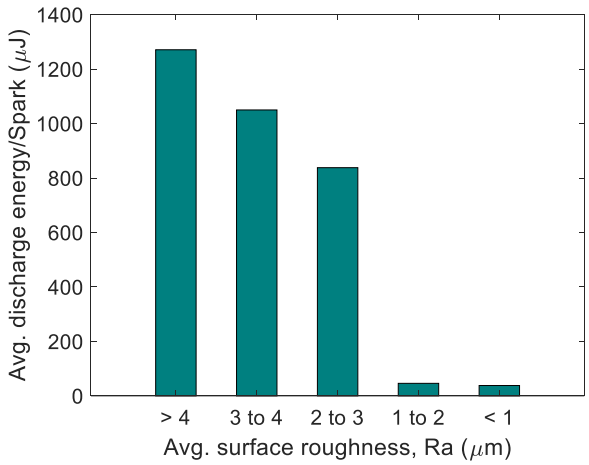

Fig. 15. Effect of discharge energy on the surface roughness

The current study was performed on an Inconel plate of uniform thickness. In case of offline models, the input parameters are related to the process responses and will only give accurate results for the workpiece thickness considered. But, since the current study proposes an online model, the external factors like increased workpiece thickness should reflect on the discharge characteristics like discharge energy, pulse frequency and abnormal pulse proportions. Thus, the model is designed to be robust to such external factors.

However, an extensive study on such factors (like effect of complexity of machined profile and workpiece thickness) is planned as a future work. Also, the processing time (response delay) for failure prediction and control is dependent on the computing power of PC and data transfer rate of the DAQ.

3.3 Comparison with existing condition monitoring models

A comparison of the capabilities of the proposed model with respect to currently available literature on condition monitoring systems is given in this section. While many of the models developed in the past are capable of wire break prediction (Kwon and Yan, 2006; Cabanes et al., 2008), spark absence and similar other failures that affects the process efficiency were unaddressed. Also, many prediction models in the past does not come up with an associated process control algorithm (Kwon and Yan, 2006; Cabanes et al., 2008; Kumar and Choudhury, 2011; Kumar et al., 2013). The process control models which are not based on pulse classification may not be identifying/addressing the machining instabilities caused by abnormal pulses (Mendes et al., 2014; Zhidong et al., 2014; Bufardi et al., 2015). Several other works are dedicated to only feature extraction or pulse classification techniques (Caggiano et al.,

2018; Obwald et al., 2018; Conde et al., 2018; Bergs et al.,2018). Also, many of the past failure detection models have not discussed the surface integrity improvements offered by their process control algorithms.

The proposed model is capable of online feature extraction (of relevant discharge characteristics), pulse classification, failure alert, severity assessment and intelligent process control. Additionally, in this study, the process control algorithm demonstrates a reasonable surface integrity improvement over the unstable machining conditions.

4. Conclusions

The study presents a process failure detection and control algorithm for wire electric discharge machining process to improve its efficiency and productivity. A condition monitoring system involving differential and current probes extract voltage and current waveforms during the machining. To cover all aspects of machining instabilities, a novel multi-step control strategy is proposed. The model can be considered as an improvement over the existing models which either predicts just the wire breakage, or is not pulse classification based, or is not having a process control system. Also, the proposed model has additionally reported an improvement in surface integrity, which most of the existing models have failed to analyse.

The proposed method is based on the extracted discharge characteristics like discharge energy, spark frequency and pulse proportions. These characteristics are observed to display distinguishable variations during the conditions leading to machining failures. The type of failure is predicted based on these extracted features, after which, the severity of the wire breakage failure is assessed. According to the severity of process instability, the algorithm recommends revised process parameters to restore the machining stability and to avoid the predicted failures. The process control was observed to result in failure free operation by establishing normal discharge pulse cycle, from unideal short circuit and open circuit dominated pulse cycles. Additionally, the part quality of the machined surfaces was also enhanced by the revised conditions.

Appendix

Table 7. Experimental details

S. No.	Pulse on time (µs)	Pulse off time (µs)	Servo voltage (V)	Input current (A)	Discharge energy (µJ)	SPARK v (Hz)	NSR	OSR	ASR + SSR	Cutting speed (mm/min)	Ra (µm)	Machining outcome
1	105	30	30	40	613.68	75000	0.11	0.05	0.84	1.88	3.68	WB
2	105	30	50	40	508.20	41000	0.18	0.29	0.52	1.16	3.24	NM
3	105	40	30	40	544.43	52000	0.41	0.15	0.43	1.47	3.70	NM
4	105	40	50	40	560.02	26000	0.12	0.48	0.40	0.83	2.80	NM
5	105	50	30	40	548.51	28500	0.28	0.30	0.42	0.77	2.65	NM
6	105	50	50	40	583.22	14000	0.07	0.57	0.36	0.47	2.29	NM
7	110	30	30	40	1044.30	26500	0.25	0.32	0.43	2.60	3.92	WB
8	110	30	50	40	1066.32	45000	0.28	0.28	0.44	2.40	4.10	WB
9	110	40	30	40	1033.86	22500	0.27	0.40	0.33	1.70	3.77	NM
10	110	40	50	40	986.55	29000	0.17	0.29	0.53	1.61	3.54	WB
11	110	50	30	40	1123.73	16000	0.06	0.53	0.41	1.58	3.56	NM
12	110	50	50	40	1002.03	20500	0.15	0.32	0.54	0.84	3.87	WB
13	115	30	30	40	1476.84	22500	0.15	0.26	0.59	2.70	4.33	WB
14	115	30	50	40	1596.05	9000	0.00	0.89	0.11	1.29	3.29	NM
15	115	40	30	40	1484.71	25500	0.10	0.10	0.75	1.87	3.97	WB
16	115	40	50	40	1646.00	11500	0.09	0.74	0.17	1.04	2.93	NM
17	115	50	30	40	1618.15	11500	0.30	0.52	0.17	1.31	3.25	NM
18	115	50	50	40	1658.98	5000	0.10	0.70	0.20	0.70	2.32	NM
19	105	30	30	10	56.68	65000	0.29	0.11	0.60	0.32	1.94	NM
20	105	30	50	10	76.66	24500	0.33	0.31	0.37	0.2	1.07	NM
21	105	40	30	10	34.92	34000	0.43	0.31	0.26	0.24	1.43	NM
22	105	40	50	10	47.62	12000	0.29	0.58	0.13	0.14	-	SA
23	105	50	30	10	32.06	13500	0.08	0.31	0.03	0.14	-	SA
24	105	50	50	10	42.60	19500	0.18	0.44	0.38	0.06	-	SA
25	110	30	30	10	40.62	6500	0.38	0.23	0.38	0.38	1.80	NM
26	110	30	50	10	45.23	39500	0.22	0.30	0.48	0.23	1.23	NM
27	110	40	30	10	38.61	43500	0.39	0.16	0.45	0.27	1.30	NM
28	110	40	50	10	22.78	37500	0.33	0.25	0.41	0.16	0.96	NM
29	110	50	30	10	52.52	21000	0.21	0.38	0.40	0.17	0.93	NM
30	110	50	50	10	42.55	14500	0.10	0.45	0.45	0.1	-	SA
31	115	30	30	10	34.65	67000	0.31	0.11	0.58	0.44	2.07	NM
32	115	30	50	10	60.84	32000	0.50	0.33	0.17	0.25	1.45	NM
33	115	40	30	10	22.37	57500	0.12	0.05	0.83	0.33	1.69	NM
34	115	40	50	10	38.98	19500	0.26	0.31	0.44	0.18	0.82	NM
35	115	50	30	10	40.56	22500	0.33	0.38	0.29	0.23	1.39	NM
36	115	50	50	10	65.58	15500	0.35	0.48	0.16	0.09	-	SA

WB – Wire breakage, CM - Continuous machining,
NSR- Normal spark ratio, ASR- Arc spark ratio, SSR- Short spark ratio, OSR- Open spark ratio

References

1. Ho KH, Newman ST, Rahimifard S, Allen RD. State of the art in wire electrical discharge machining (WEDM). Int J Mach Tools Manuf 2004; 44:1247–59. https://doi.org/10.1016/j.ijmachtools.2004.04.017.
2. Mandal A, Dixit AR. State of art in wire electrical discharge machining process and performance. Int J Mach Mach Mater 2014; 16:1. https://doi.org/10.1504/IJMMM.2014.063918.
3. Gamage JR, Desilva AKM. Effect of Wire Breakage on the Process Energy Utilisation of EDM. Procedia CIRP 2016; 42:586–90. https://doi.org/10.1016/j.procir.2016.02.264.
4. Hewidy MS, El-Taweel TA, El-Safty MF. Modelling the machining parameters of wire electrical discharge machining of Inconel 601 using RSM. J Mater Process Technol 2005; 169:328–36. https://doi.org/10.1016/j.jmatprotec.2005.04.078.
5. Aggarwal V, Khangura SS, Garg RK. Parametric modeling and optimization for wire electrical discharge machining of Inconel 718 using response surface methodology. Int J Adv Manuf Technol 2015; 79:31–47. https://doi.org/10.1007/s00170-015-6797-8.
6. Senkathir S, Aravind R, Samson RM, Raj ACA. Optimization of Machining Parameters of Inconel 718 by WEDM Using Response Surface Methodology. Adv Manuf Process 2019:383–92. https://doi.org/10.1007/978-981-13-1724-8.
7. Gautier G, Priarone PC, Rizzuti S, Settineri L, Tebaldo V. A contribution on the modelling of wire electrical discharge machining of a γ-TiAl alloy. Procedia CIRP 2015; 31:203–8. https://doi.org/10.1016/j.procir.2015.03.019.
8. Cabanes I, Portillo E, Marcos M, Sánchez JA. An industrial application for on-line detection of instability and wire breakage in wire EDM. J Mater Process Technol 2008; 195:101–9. https://doi.org/10.1016/j.jmatprotec.2007.04.125.
9. Fedorov AA, Blesman AI, Postnikov D V., Polonyankin DA, Russkikh GS, Linovsky A V. Investigation of the impact of Rehbinder effect, electrical erosion and wire tension on wire breakages during WEDM. J Mater Process Technol 2018; 256:131–44. https://doi.org/10.1016/j.jmatprotec.2018.02.002.
10. Okada A, Konishi T, Okamoto Y, Kurihara H. Wire breakage and deflection caused by nozzle jet flushing in wire EDM. CIRP Ann - Manuf Technol 2015; 64:233–6. https://doi.org/10.1016/j.cirp.2015.04.034.
11. Luo YF. Rupture failure and mechanical strength of the electrode wire used in wire EDM. J Mater Process Technol 1999; 94:208–15. https://doi.org/10.1016/S0924-0136(99)00107-7.
12. K. P. Rajurkar; W. M. Wang. On-Line Monitor and Control for Wire Breakage in WEDM. Ann CIRP 1991; 40:219–22. https://doi.org/10.1016/j.procir.2017.12.059.
13. Kwon S, Yang MY. The benefits of using instantaneous energy to monitor the transient state of the wire EDM process. Int J Adv Manuf Technol 2006; 27:930–8.

https://doi.org/10.1007/s00170-004-2252-y.

14. Liao YS, Woo JC. Design of a fuzzy controller for the adaptive control of WEDM process. Int J Mach Tools Manuf 2000; 40:2293–307. https://doi.org/10.1016/S0890-6955(00)00036-5.
15. Bufardi A, Akten O, Arif M, Xirouchakis P. Towards zero-defect manufacturing with a combined online - offline fuzzy-nets approach in wire electrical discharge machining 2017:401–9.
16. Yan MT, Liao YS. A self-learning Fuzzy controller for wire rupture prevention in WEDM. Int J Adv Manuf Technol 1996; 11:267–75. https://doi.org/10.1007/BF01351284.
17. Lin C-T, Chung I-F, Huang S-Y. Improvement of machining accuracy by fuzzy logic at corner parts for wire-EDM. Fuzzy Sets Syst 2001; 122:499–511.
18. Conde A, Sanchez JA, Plaza S, Ostolaza M, De La Puerta I, Li Z. Experimental Measurement of Wire-lag Effect and Its Relation with Signal Classification on Wire EDM. Procedia CIRP 2018; 68:132–7. https://doi.org/10.1016/j.procir.2017.12.035.
19. Janardhan V, Samuel GL. Pulse train data analysis to investigate the effect of machining parameters on the performance of wire electro discharge turning (WEDT) process. Int J Mach Tools Manuf 2010; 50:775–88. https://doi.org/10.1016/j.ijmachtools.2010.05.008.
20. Oßwald K, Lochmahr I, Schulze H-P, Kröning O. Automated Analysis of Pulse Types in High-Speed Wire EDM. Procedia CIRP 2018; 68:796–801. https://doi.org/10.1016/j.procir.2017.12.157.
21. Abhilash, P. M. Chakradhar D. Prediction and analysis of process failures by ANN classification during wire-EDM of Inconel 718. Adv Manuf 2020; 8:519–36. https://doi.org/10.1007/s40436-020-00327-w.
22. Abhilash PM, Chakradhar D. ANFIS modelling of mean gap voltage variation to predict wire breakages during wire EDM of Inconel 718. CIRP J Manuf Sci Technol 2020; 31:153–64. https://doi.org/10.1016/j.cirpj.2020.10.007.
23. Newton TR, Melkote SN, Watkins TR, Trejo RM, Reister L. Investigation of the effect of process parameters on the formation and characteristics of recast layer in wire-EDM of Inconel 718. Mater Sci Eng A 2009;513–514:208–15. https://doi.org/10.1016/j.msea.2009.01.061.
24. Klocke F, Welling D, Klink A, Perez R. Quality assessment through in-process monitoring of wire-EDM for fir tree slot production. New Prod Technol Aerosp Ind - 5th Mach Innov Conf (MIC 2014)-Procedia CIRP 2014; 24:97–102. https://doi.org/10.1016/j.procir.2014.07.136.
25. Caggiano A, Teti R, Perez R, Xirouchakis P. Wire EDM monitoring for zero-defect manufacturing based on advanced sensor signal processing. Procedia CIRP 2015; 33:315–20. https://doi.org/10.1016/j.procir.2015.06.065.
26. Mwangi JW, Bui VD, Thüsing K, Hahn S, Wagner MF-X, Schubert A. Characterization of the arcing phenomenon in micro-EDM and its effect on key mechanical properties of medical-grade Nitinol. J Mater Process Technol 2020; 275:116334.

27. Kumar A, Kumar V, Kumar J. Parametric Effect on Wire Breakage Frequency and Surface Topography in WEDM of Pure Titanium. J Mech Eng Technol 2013;1:51–6. https://doi.org/10.18005/jmet0102003.
28. Kumar R, Choudhury SK. Prevention of wire breakage in wire EDM. Int J Mach Mach Mater 2011;9:86–102. https://doi.org/10.1504/IJMMM.2011.038162.
29. Ramamurthy A, Sivaramakrishnan R, Muthuramalingam T, Venugopal S. Performance Analysis of Wire Electrodes on Machining Ti-6Al-4V Alloy using Electrical Discharge Machining Process. Mach Sci Technol 2015;19:577–92. https://doi.org/10.1080/10910344.2015.1085314.
30. Maher I, Sarhan AAD, Hamdi M. Review of improvements in wire electrode properties for longer working time and utilization in wire EDM machining. Int J Adv Manuf Technol 2014;76:329–51. https://doi.org/10.1007/s00170-014-6243-3.
31. Abhilash, P.M., Chakradhar, D. Sustainability improvement of WEDM process by analysing and classifying wire rupture using kernel-based naive Bayes classifier. J Braz. Soc. Mech. Sci. Eng. 43, 64 (2021). https://doi.org/10.1007/s40430-021-02805-z
32. Kwon S, Lee S, Yang M. Experimental investigation of the real-time micro-control of the WEDM process. Int J Adv Manuf Technol 2015;79:1483–92. https://doi.org/10.1007/s00170-015-6903-y.
33. Bergs T, Tombul U, Herrig T, Olivier M, Klink A, Klocke F. Analysis of Characteristic Process Parameters to Identify Unstable Process Conditions during Wire EDM. Procedia Manuf 2018;18:138–45. https://doi.org/10.1016/j.promfg.2018.11.018.
34. Pramanik A, Basak AK. Sustainability in wire electrical discharge machining of titanium alloy: Understanding wire rupture. J Clean Prod 2018;198:472–9. https://doi.org/10.1016/j.jclepro.2018.07.045.
35. Sharma P, Chakradhar D, Narendranath S. Evaluation of WEDM performance characteristics of Inconel 706 for turbine disk application. Mater Des 2015;88:558–66. https://doi.org/10.1016/j.matdes.2015.09.036.
36. Zhidong L, Haoran C, Huijun P, Mingbo Q, Zongjun T. Automatic control of WEDM servo for silicon processing using current pulse probability detection. Int J Adv Manuf Technol 2014;76:367–74. https://doi.org/10.1007/s00170-014-6252-2.
37. Mendes LA, Amorim FL, Weingaertner WL. Automated system for the measurement of spark current and electric voltage in wire EDM performance. J Brazilian Soc Mech Sci Eng 2014;37:123–31. https://doi.org/10.1007/s40430-014-0171-x.
38. Abhilash PM, Chakradhar D. Surface integrity comparison of wire electric discharge machined Inconel 718 surfaces at different machining stabilities. Procedia CIRP 2020;87:228–33. https://doi.org/10.1016/j.procir.2020.02.037.